On Strategies for Predictive Shock-Driven Turbulent Mixing Simulation

Fernando F. Grinstein
Applied Physics Division, Los Alamos National Laboratory
MS B259, Los Alamos, NM 87545, USA
fgrinstein@lanl.gov

Abstract. In the large eddy simulation (LES) approach large-scale energy-containing structures are resolved, smaller (presumably) more isotropic structures are filtered out, and unresolved subgrid effects are modeled. Extensive recent work has demonstrated that predictive simulations of turbulent velocity fields are possible based on subgrid scale modeling implicitly provided by high-resolution finite-volume numerical algorithms. This strategy is called implicit LES. The extension of the approach to the substantially more difficult problem of material mixing is addressed, and progress in representative (shock-driven) mixing studies is reported.

Keywords:. ILES, MILES, shock-driven, turbulent mixing,

I Introduction

It is not feasible to compute high Reynolds-number (Re) turbulent flows by directly resolving all scales of motion and material interfaces; instead, macroscale portions of the unsteady turbulent motion are computed while the rest of the flow physics including molecular diffusion and other microscale physics (e.g., combustion) remains unresolved. In large eddy simulation (LES) [1] the large energy containing structures are resolved whereas the smaller, presumably more isotropic, structures are filtered out and their unresolved subgrid scale (SGS) effects are modeled. The construction of SGS models for LES is pragmatic and based primarily on empirical information. Adding to the physics based difficulties in developing and validating SGS models, truncation terms due to discretization are comparable to SGS models in typical LES strategies [2], and LES resolution requirements become prohibitively expensive for practical flows and regimes. Implicit LES [3] (ILES) – and monotone integrated LES (MILES) introduced earlier [4] – effectively address the seemingly insurmountable issues posed to LES by under-resolution, by relying on the use of SGS modeling and filtering provided implicitly by physics capturing numerics.

Extensive work has demonstrated that predictive unresolved simulations of turbulent velocity fields are possible using a class of high resolution, non-oscillatory finite-volume (NFV) numerical algorithms [3,5-8]. This is a new area of research undergoing rapid evolution; scientific understanding and theory explaining the success of these methods have been proposed; truncation terms associated with NFV methods implicitly provide SGS models capable of emulating the physical dynamics of the unresolved turbulent velocity fluctuations by themselves; connection of these

truncation terms to the physical theory of inviscid dissipation and ultimately to irreversible thermodynamics has been recently demonstrated [8]. Popular NFV methods such as flux-corrected transport (FCT), the piecewise parabolic method (PPM), total variation diminishing (TVD), and hybrid algorithms are being used for ILES. Extensive ILES verification and validation in areas of engineering, geophysics, and astrophysics has been reported [3]. The extension of the approach to the substantially more difficult problem of material mixing is addressed in the present paper, and progress in representative (shock-driven) mixing studies is reported.

II Implicit Large Eddy Simulation

The ILES strategy uses truncation terms of certain numerical methods to account for the accumulated effects of unresolved motions at the large scales and to emulate the SGS physics. The understanding of ILES methods is primarily based on a formal procedure called modified equation analysis (MEA) [5,6]. Conceptually, the simplest material mixing case to discuss is that of incompressible flow with passive scalar mixing. In symbolic form, the corresponding modified LES equations (satisfied by the numerically calculated solutions) are

$$\partial_t(\bar{\mathbf{v}}) + \nabla\cdot(\bar{\mathbf{v}}\otimes\bar{\mathbf{v}}) + \nabla\bar{p} - \nu\nabla\cdot\bar{\mathbf{S}} = -\nabla\cdot\boldsymbol{\sigma}_{\mathbf{v}} + \mathbf{t}_{\mathbf{v}}$$
$$\partial_t(\theta) + \nabla\cdot(\bar{\theta}\bar{\mathbf{v}}) - \kappa\nabla^2\bar{\theta} = -\nabla\cdot\boldsymbol{\sigma}_{\theta} + \mathbf{t}_{\theta}\ ,$$

where the bar denotes a formal spatial filtering procedure, $\mathbf{v}$ is the (solenoidal) velocity field, θ is a conserved material scalar concentration, ν and κ denote momentum and material diffusivity, respectively. To ensure closure of the equations in the filtered unknowns, explicit models for $\boldsymbol{\sigma}_{\mathbf{v}} = \overline{\mathbf{v}\otimes\mathbf{v}} - \bar{\mathbf{v}}\otimes\bar{\mathbf{v}}$ and $\boldsymbol{\sigma}_{\theta} = \overline{\theta\,\mathbf{v}} - \bar{\theta}\bar{\mathbf{v}}$ have to be provided. In typical LES strategies, $\mathbf{t}_{\mathbf{v}}$ and $\mathbf{t}_{\theta}$ – truncation terms due to discretization and filtering, have contributions directly comparable with those of the explicit models [2]. ILES minimizes such competition, by relying only on the implicit SGS modeling and filtering provided by the numerics. *Good or bad SGS physics can be designed into the ILES depending on the choice of numerics*. MEA provides a framework to reverse engineer physically desirable features into the numerics design [3].

For regimes driven by large scale flow features – which LES is designed to model, implicit models associated with NFV methods have been shown to be capable by themselves ($\sigma\equiv 0$) to emulate SGS physics effects on statistics of turbulent velocity fluctuations [3]. Major features of the flow physics can be captured with locally adaptive (dynamic) NFV numerics: 1) the small-scale anisotropy of high-Re turbulent flows (e.g., line vortices, shocks), 2) the viscosity-independent dissipation characteristic of the turbulent cascade, 3) the inherently discrete dynamics of (finite scale) laboratory observables. By focusing on inertially dominated flow dynamics and regularization of the under-resolved flow, ILES follows on the precedent of using

NFV methods for shock capturing – requiring weak solutions and satisfaction of an entropy condition.

As with any LES, additional explicit SGS modeling ($\sigma \neq 0$) may be needed with ILES to address SGS driven flow features (e.g., backscatter, scalar mixing, and chemical reaction). The extension of the LES approach to the substantially more difficult problem of under-resolved material mixing by an under-resolved velocity field has not yet been investigated numerically nor are there theories as to when such a methodology may be successful. A major research focus is on evaluating the extent to which SGS physical material mixing effects can be implicitly modeled as the turbulent velocity fluctuations, recognizing when additional material numerical treatments are needed, and developing a sound conceptual and analytical framework for designing effective SGS modeling strategies for complex turbulent mixing simulations using *mixed* explicit-implicit SGS modeling contributions acting in effective *collaborative* (rather than competitive) fashion.

III Shock-Driven Turbulent Mixing

In many applications of interest, turbulence is generated by shock waves via Richtmyer-Meshkov instabilities (RMI) (e.g., [9]). The instability results in vorticity being introduced at material interfaces by the impulsive loading of the shock wave. A critical feature of this impulsive driving is that the turbulence decays as dissipation removes kinetic energy from the system. RMI add the complexity of shock waves and other compressible effects to the basic physics associated with mixing; compressibility further affects the basic nature of material mixing when mass density and material mixing fluctuation effects are not negligible. Because RMI are shock-driven, resolution requirements make direct numerical simulation impossible even on the largest supercomputers. State-of-the-art simulations of RMI instabilities (e.g., [10]) use hybrid methods which use adaptive mesh refinement and switch between shock capturing schemes and conventional LES depending on the local flow conditions. Given that ILES is based on locally adaptive NFV methods it is naturally suited to emulate shock physics. The unique combination of shock and turbulence emulation capabilities supports direct use of ILES as an effective simulation *anzatz* in RMI research. This possibility is demonstrated in the current paper in the context of a prototypical case study for which available laboratory data [9] and previous LES [10] can be used to test and validate ILES modeling based on NFV methods.

The present simulations use ILES to model shock-tube experiments performed by Vetter and Sturtevant [9] involving various combinations of high- (SF_6) and low-density (air) gases, shock directions, positions of the membrane and the wire mesh initially separating the gases, and reshock off an endwall. In the particular simulations considered here the shock initially passes from the low- to the high-density fluids, and the membrane is initially on the same side of the mesh as the shock; mixing-layer growth is affected by the initial interaction of shock and material-interface (with direct distinct imprint of the mesh spacing on the initial contact discontinuity shape), and significant further effects occur after reshock. We model the experimental setup approximately as follows. The air-SF_6 contact discontinuity is modeled as a discontinuity in density of a single ideal gas with a ratio of specific heats

1.3. The temperature changes appropriately so as to maintain a constant pressure across the initial interface. A shock is created by moving this fluid into a higher-density, higher-pressure region where density and pressure discontinuities are chosen to satisfy the Rankine-Hugoniot relations for a Mach 1.5 shock. The simulations are carried out in a reference frame in which the air-SF_6 interface is initially at rest. The shock propagates through the contact discontinuity and reflects at the end of the simulation box (Fig.1).

In addition to SGS modeling issues discussed above, flow and material transport equations must be supplemented by initial and boundary conditions to fully pose the turbulent flow problem of interest. Inherent difficulties with the open problem of predictability of material stirring and molecular mixing by under-resolved numerically generated multi-scale turbulent velocity fields, are compounded with the inherent sensitivity of turbulent flows to initial conditions (IC's) [11]. Thus, a crucial issue when simulating turbulent flows such as considered here is that of modeling the (insufficiently characterized) initial contact discontinuity deformation in the experiments. The surface displacement of the interface is modeled here as follows:

$$\Delta x = \alpha\left[\,|\sin(10\pi y)\sin(10\pi z)| - \sin(2\pi y)\sin(2\pi z) + R(x,y,z)\right]$$

,

S L *R*

where α is a parameter (chosen to be α=0.27cm as in [12]), and x denotes the streamwise (shock propagation) direction. A short (S) wavelength deformation is chosen to represent the result of pushing the membrane through the wire mesh, and is superimposed to the distortion of the wire mesh on the longer (L) scale of the shock tube transverse dimension; an added random perturbation (R) varies in amplitude between 0-1 at each grid point. Interface deformation treatments in previously reported relevant work were based on short/long models of the type S+L [12], or non-deterministic short/random S+R [10] expressions, respectively. Periodic boundary conditions are imposed in the tranverse (y,z) directions. The particular ILES strategy tested here is based on a nominally-inviscid simulation model (e.g., [5]) which solves the conservation equations for mass density (ϱ), momenta (ϱui), total energy, and SF_6 mass density ϱ_{SF6} (convected as a separate scalar); a predictor-corrector directional-split 4th-order FCT algorithm is used on uniformly-spaced computational grids with mesh spacing h in the range 0.05-0.2cm.

Cross-stream average quantities used in the analysis below are defined as follows

$$\langle f\rangle(x) = \frac{1}{A}\int f(x,y,z)dydz \;\;,\;\; A = \int dydz$$

$$\rho = \langle \rho \rangle + \rho',$$
$$\tilde{u}_i = \langle \rho u_i \rangle / \langle \rho \rangle,$$
$$u_i = \langle u_i \rangle + u_i' = \tilde{u}_i + u_i'' ,$$
$$\mathrm{R}_{ij} = \left\langle \rho u_i'' u_j'' \right\rangle,$$
$$r_{ij} = \langle \rho \rangle \left\langle u_i' u_j' \right\rangle,$$
$$2\tilde{k} = \mathrm{R}_{mm},$$
$$2\langle k \rangle = r_{mm},$$
$$\psi = \left\langle \frac{\rho_{SF_6}}{\rho} \right\rangle,$$

where the tilde denotes mass-weighted (*Favre*) averaging, summation over repeated indices is assumed, R and r are Reynolds stress, *k* denotes turbulent kinetic energy, and Ψ is the mixedness.

The approximate wave diagram in Fig.2 depicting the evolution and interaction of the M=1.5 shock and air/SF6 interface for a selected case (3D, S+R), is in good agreement with similar diagrams in other cases here and in the previous work [9,10]. The mixing layer is first hit by the shock around 0.0007 sec, and then by reshock after 0.003 sec. Corresponding statistical analysis of the mixing layer evolution is presented in Figs. 3, in terms of mixedness and turbulent kinetic energy characteristic measures. Mixedness width (Fig.3a) and peak turbulent kinetic energy (Fig.3bc) increase drastically after reshock, with the profiles of k exhibiting decay and broadening at later times (Fig.3c). Favre turbulent kinetic energy predictions are half as large as non mass-weighted predictions just after reshock (t=0.0036 sec), but appear more comparable for later times.

Typical two-dimensional visualizations of distributions of the SF6 mass fraction ϱSF6/ϱ illustrating the RMI evolution are shown on Fig.4 for the S+L case and h=0.05-0.1cm; instantaneous results from the 3D (410x135x135) simulations using h=0.2cm are shown on Fig.5 for the various different IC cases considered. Representative results of spectral velocity fluctuation analysis performed on 64x128x128 data sub-volumes chosen around the mixing layer centerplanes are presented in Fig.6 for the non-deterministic cases (S+R, L+S+R). The instantaneous velocity fluctuation is de¬com¬posed into its solenoidal and compressible components according to $\mathbf{v}=\mathbf{v}^s+\mathbf{v}^c$, with the condition $\nabla\cdot(\mathbf{v}^s)=0$ in physical space translating into the condition $\mathbf{k}\cdot\hat{\mathbf{v}}^s=0$ in Fourier space. This condition is explicitly used to separate solenoidal and compressible components of the Fourier velocity transform in the form $\hat{\mathbf{v}}^s = \hat{\mathbf{v}} - \hat{\mathbf{v}}^c$ with $\hat{\mathbf{v}}^c = (\hat{\mathbf{v}} \cdot \mathbf{k})\mathbf{k} / |\mathbf{k}|^2$. Figure 6 indicates significantly larger solenoidal components as the flow becomes turbulent as indicated

by a short Kolmogorov $k^{-5/3}$ inertial range. Consistent, with these results, the comparable *Favre* and non mass-weighted turbulent kinetic energy predictions for the late times (Fig.3c), suggest that mass density fluctuation effects are somewhat less important as turbulence develops after reshock.

Predicted measures of the mixing thickness are compared with the experiments [9] and previous simulations [10] in Fig. 7. The mixing thickness θ is defined here as in [10],

$$\theta = 4\int \psi(x)[1-\psi(x)]dx \ .$$

At initialization (t=0), the initial interface perturbation (not yet affected by the shock) is apparent in the top frames in Fig.4; by the next frames (t=2.2ms) the mixing layer has been shocked, and later reshock reflects (as noted) on significantly faster mixing layer growth, e.g., slope of the predicted mixing thickness between 3-5ms on Fig.7.
We find good agreement on the statistical mix measures between present ILES predictions, experiments, and previous simulations (Fig.7). Two-dimensional simulations are found to be adequate for early times, but they predict significantly slower mixing growth after reshock, indicating the importance of 2D-unaccounted vortex stretching dynamics and transition to turbulence effects. The 3D results become fairly independent of the choice of initial interface conditions after reshock, when the mixing layers transition to more disorganized turbulent regimes. The dependence of coherent (larger scale) vortical structures on IC's is responsible for inherently more sensitive nature of 2D predictions. Figure 7 suggests possibly higher sensitivity to IC's for later times, say, $t > 0.005$ sec when expansion effects become important (effects of new reshock due to wall-reflection of rarefaction wave produced at first reshock). Some discrepancies with the previous simulations apparent for these later times warrant further analysis – to be discussed separately – on impact of detailed prescription of IC's (similar but different S+R in [10]), grid resolution, as well as actual implementation of upstream/downstream boundary conditions.

IV Conclusions

Progress in testing and validating ILES modeling based on NFV methods in representative (shock-driven) material mixing studies are reported. A prototypical case study was considered for which laboratory data as well as LES data are available as reference. Present ILES mix predictions use relatively coarse uniform grids and no explicit SGS models. We find good agreement between ILES predictions, experiments, and previously reported simulations. Mass density fluctuation effects appear to be important at early times following initial shock-interface interaction, but less so after reshock. The work suggests that robust effective performances can be achieved with ILES in this context.

Acknowledgments

Los Alamos National Laboratory is operated by the Los Alamos National Security, LLC for the U.S. Department of Energy NNSA under Contract No. DE-AC52-06NA25396.

References

1. Sagaut P. 2006, Large Eddy Simulation for Incompressible Flows, 3rd Ed., Springer, New York.
2. Ghosal, S., 1996, An Analysis of Numerical Errors in Large-Eddy Simulations of Turbulence, J. Comput. Phys. Vol. 125, pp. 187-206.
3. F.F. Grinstein, L.G. Margolin, and W.J. Rider 2007, Eds., Implicit Large Eddy Simulation: Computing Turbulent Flow Dynamics, Cambridge University Press, New York.
4. Boris, J.P. 1990, On Large Eddy Simulation Using Subgrid Turbulence Models, in Whither Turbulence? Turbulence at the Crossroads, J.L. Lumley (editor), pp. 344-353, Springer-Verlag: New York.
5. Fureby C. & Grinstein F.F.; 2002, Large Eddy Simulation of High Reynolds-Number Free and Wall Bounded Flows, J. Comput. Phys. Vol. 181, pp. 68-97.
6. Margolin L.G. & Rider W.J. 2002, A Rationale for Implicit Turbulence Modeling, Internat. J. Numer. Methods in Fluids, Vol. 39.pp. 821-844.
7. Grinstein, F.F. and Fureby, C. 2004, From Canonical to Complex Flows: Recent Progress on Monotonically Integrated LES, Computing in Science and Engineering, Vol. 6, pp. 37-49.
8. Margolin, L.G., Rider, W.J. & Grinstein, F.F. 2006, Modeling Turbulent Flow with Implicit LES, Journal of Turbulence, Vol. 7, 015.
9. Vetter, M. & Surtevant 1995, B., Experiments on the Ritchmyer-Meshkov Instability of an Air/SF6 Interface, Shock Waves, Vol. 4, pp. 247-252.
10. Hill, D.J., Pantano, C. & Pullin, D.I. 2006, Large-Eddy Simulation and Multiscale Modelling of a Ritchmyer-Meshkov Instability with Reshock, J. Fluid Mech. Vol. 557, pp. 29–61.
11. George, WK 2006, "Recent Advancements Toward the Understanding of Turbulent Boundary Layers," AIAA Journal, Vol..44, no.11, pp.2435-2449.
12. Cohen, R.H. et al. 2002, Three-Dimensional Simulation of a Ritchmyer-Meshkov Instability with a Two-Scale Initial Perturbation, Physics of Fluids Vol. 14, pp. 3692-709.

Figure 1. Schematic of the flow configuration.

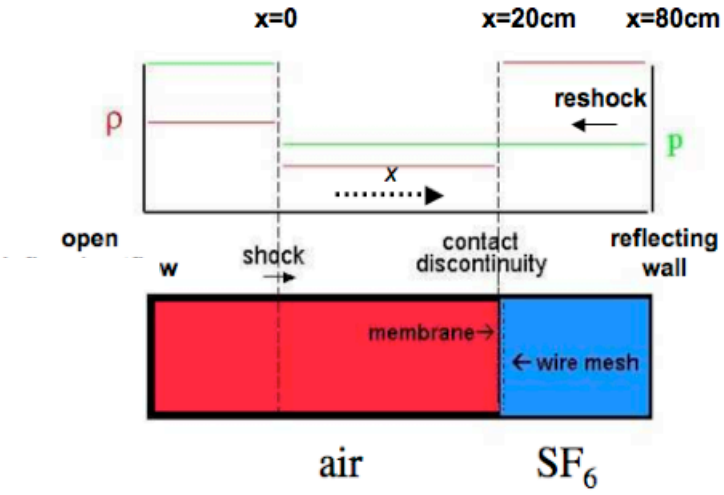

Figure 2. Approximate wave diagram depicting the evolution and interaction of the M=1.5 shock and air/SF6 interface in a representative case (3D, S+R).

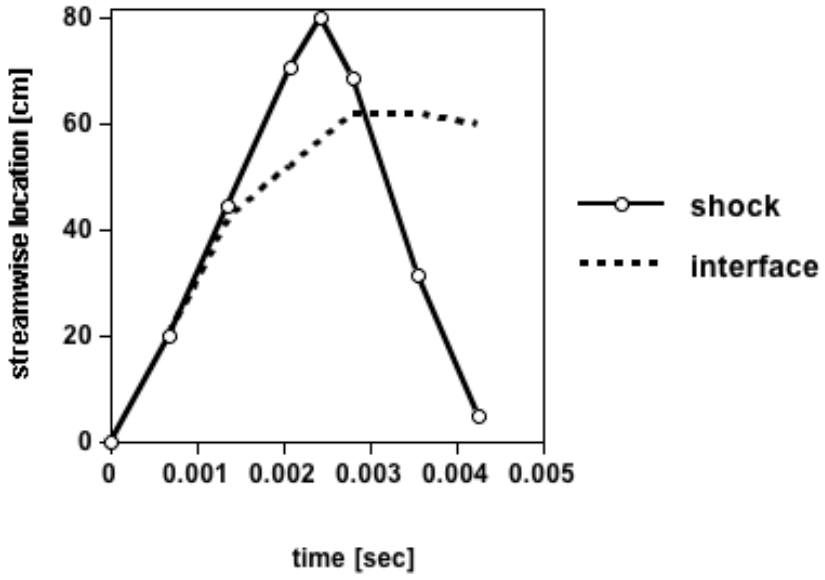

Figure 3. Statistical analysis of the mixing layer evolution in the 3D, S+R, and L+S+R cases; mixedness (top frame); turbulent kinetic energy (frames below).

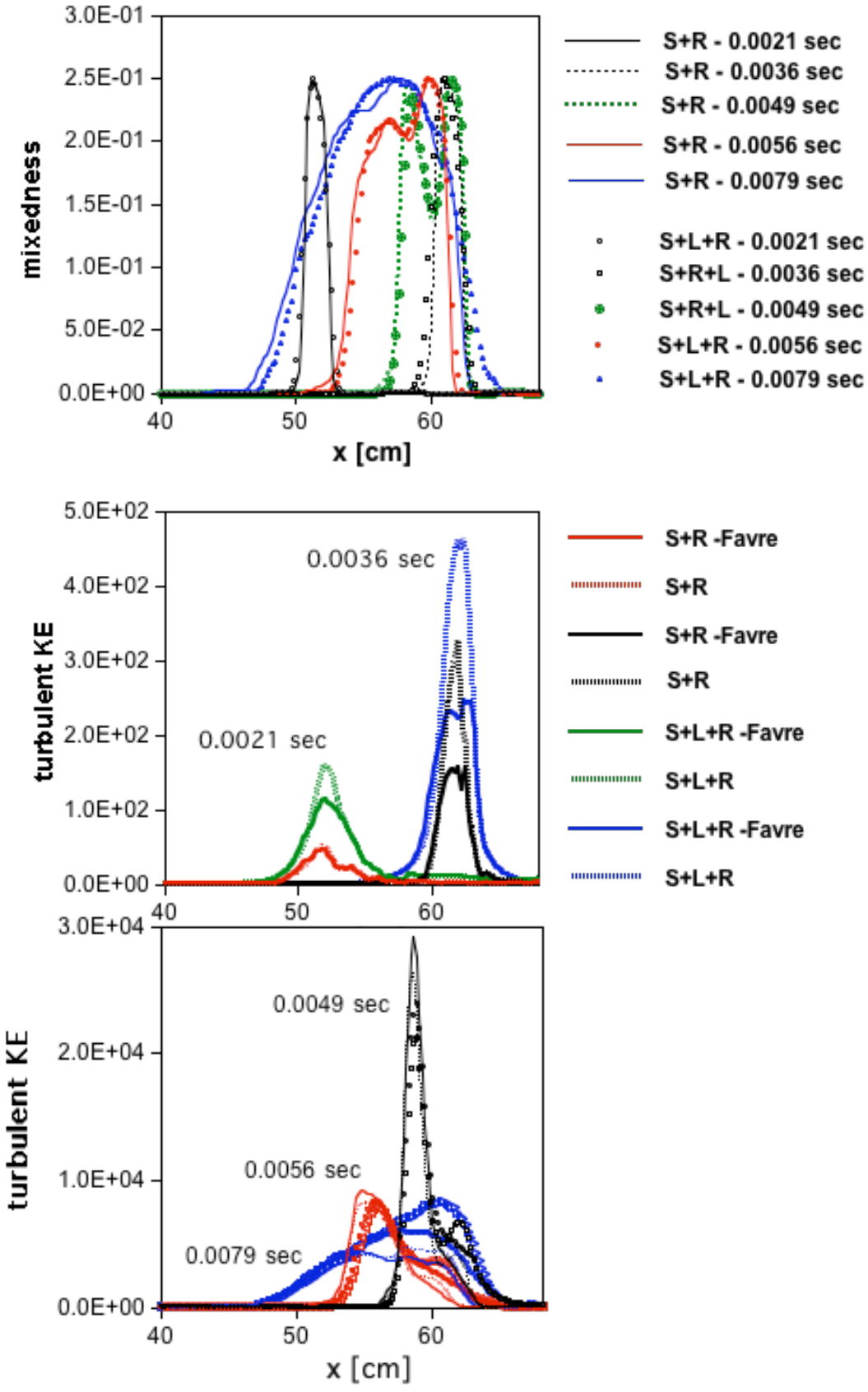

Figure 4. Typical visualizations of the SF_6 mass fraction based on 2D simulations using S+L interface modeling and uniform grid sizes h=0.1 cm (left) and h=0.05 cm (right). The simulation is initialized with the shock on the left boundary at t=0.

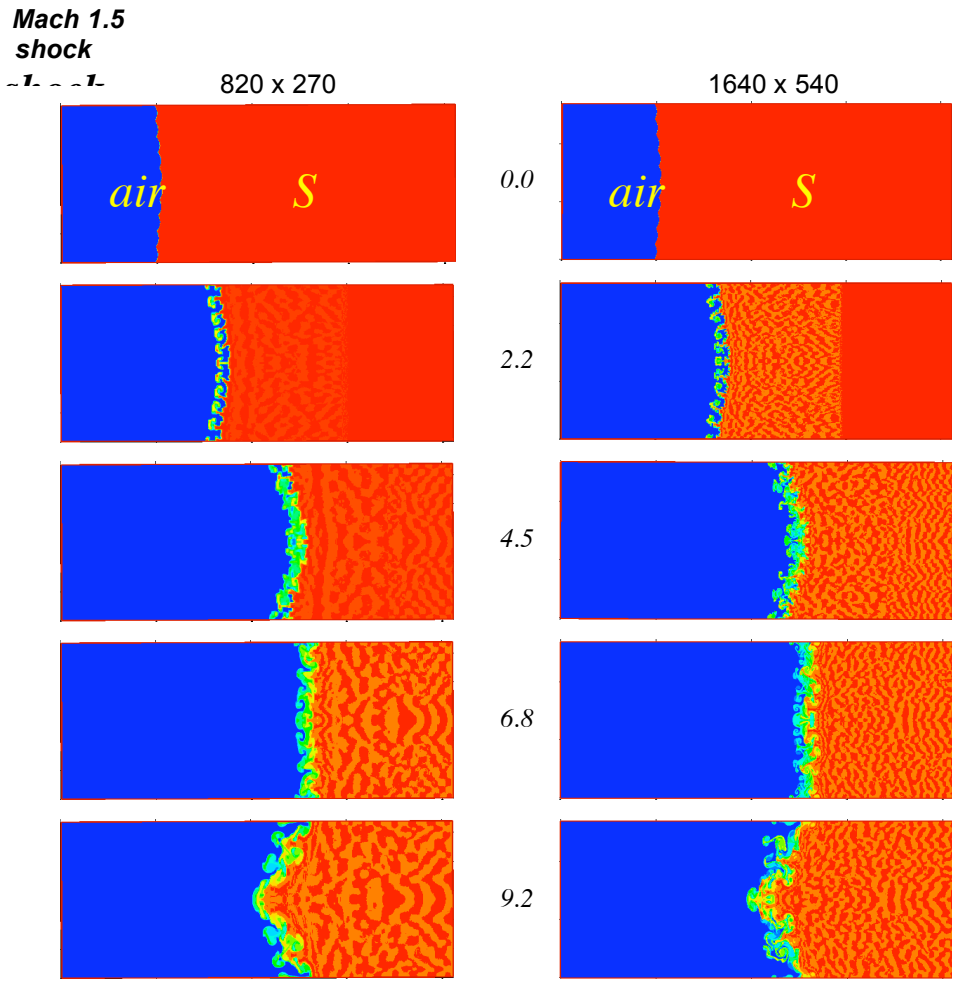

Figure 5a. Visualizations of the SF_6 mass fraction at time t = 0.009 sec, from 410x135x135 (h=0.2 cm) 3D simulations with S+L (left) and S+L+R (right) initial interface conditions.

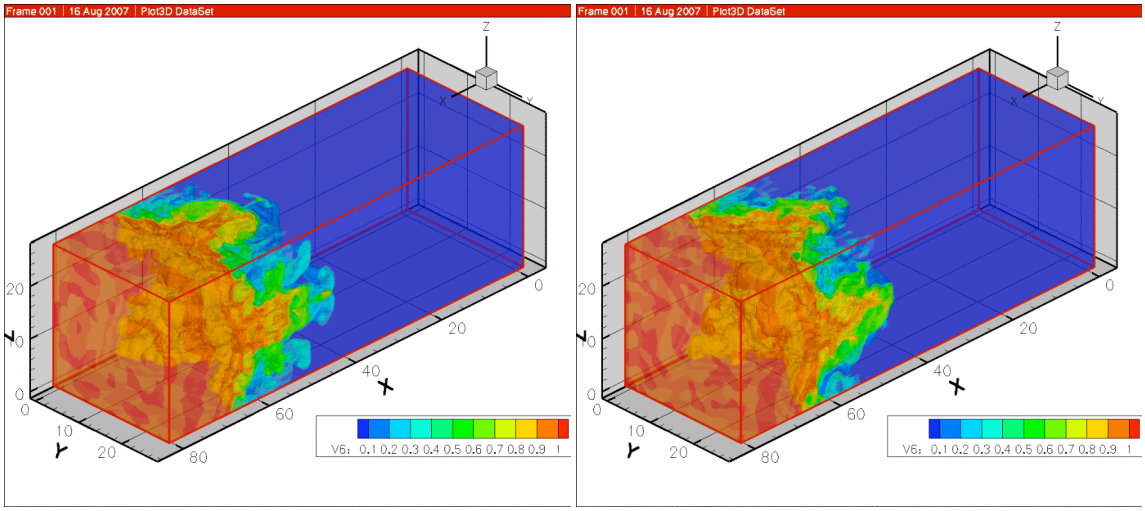

Figure 5b. Visualizations of the SF_6 mass fraction at time t = 0.009 sec, from 410x135x135 (h=0.2 cm) 3D simulations with S (left) and S+R (right) initial interface conditions.

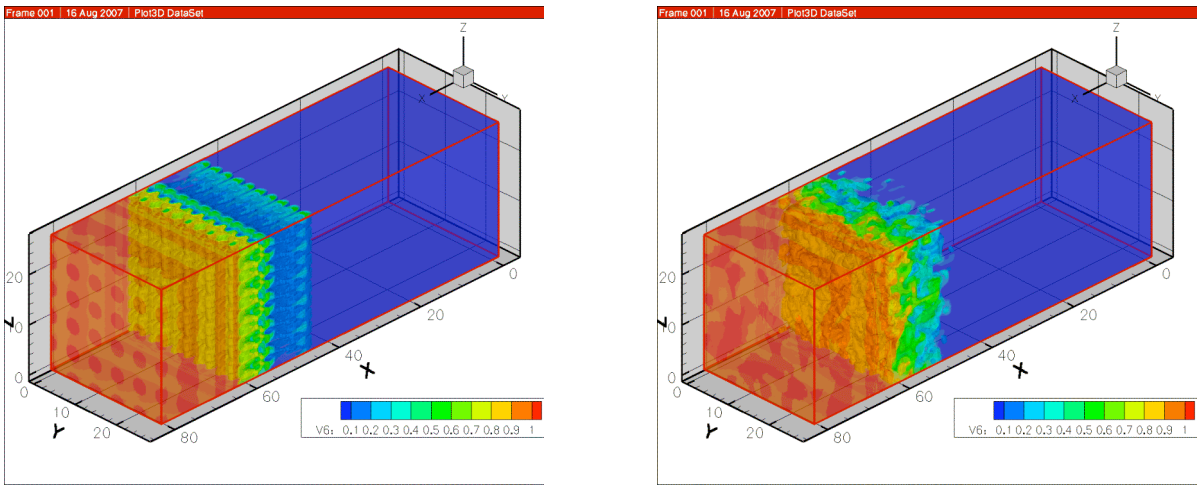

Figure 6. Developed turbulent flow kinetic energy spectra in the mixing regions for the non-deterministic cases considered (frames on the right of Fig.5).

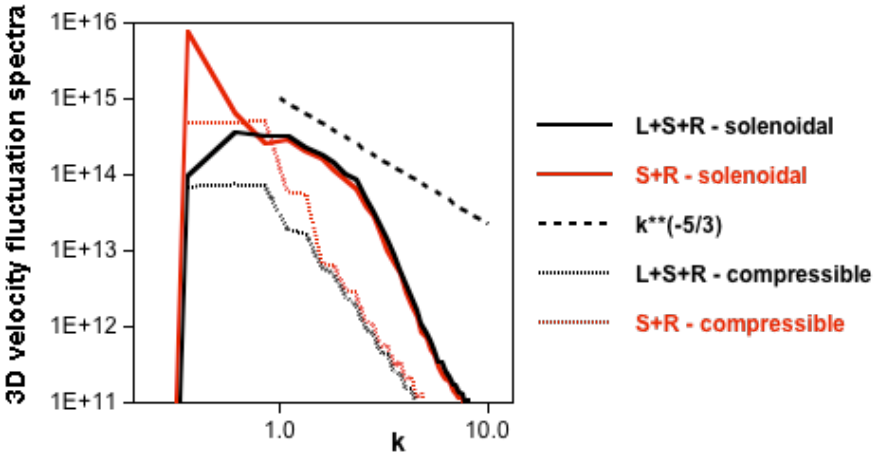

Figure 7. Predicted mixing thickness from experiments [9], previous [10] and present simulations.